Efficacy analysis of panchromatic new copper complex for visible light (455, 530 nm) radical/cationic photopolymerization: the synergic effects and catalytic cycle

Jui-Teng Lin[1,*], Jacques Lalevee[2] and Da-Chun Cheng[3,*]

. [1] New Vision Inc., Xinzhuang, New Taipei City, Taiwan; ROC;   jtlin55@gmail.com

. [2] Université de Haute-Alsace, CNRS, Mulhouse, France; jacques.lalevee@uha.fr

[3] Department of Chemistry, Qassim University, Saudi Arabia; h.tar@qu.edu.sa

. [4] Department of of Biomedical Imaging and Radiological Science, China Medical University, Taichung, Taiwan; ROC; dccheng@mail.cmu.edu.tw

* Correspondences: jtlin55@gmail.com; dccheng@mail.cmu.edu.tw

.   **Abstract**

.   This article presents, for the first time, the kinetics and the general conversion features of a 3-component system (A/B/N), based on proposed mechanism of Mau et al, for both free radical polymerization (FRP) of acrylates and the free radical promoted cationic polymerization (CP) of epoxides using various new copper complex (G2) as the initiator. Higher FRP and CP conversion can be achieved by co-additive of [B] and N, via the dual function of (i) regeneration [A], and (ii) generation of extra radicals. The FRP and CP conversion efficacy (CE) are proportional to the nonlinear power of bI[A][B], where b and I are the effective absorption coefficient and the light intensity, respectively. *In the interpenetrated polymer network (IPN) capable of initiating both FRP and CP in a blend of TMPTA and EPOX, (as the monomer for FRP and CP, respectively), the synergic effects due to CP include:: (i) CP can increase viscosity limiting the diffusional oxygen replenishment, such that oxygen inhibition effects are reduced; (ii) the cationic monomer also acts as a diluting agent for the IPN network , and (iii) the exothermic property of the CP. Many new findings are explored via our analytical formulas include: (i) the CE of FRP is about twice of the CE of CP, due to the extra radicals involved in FRP; (ii) the catalytic cycle enhancing the efficacy is mainly due to the regeneration of the initiator, and (iii) the nonlinear dependence of light intensity of the CE (in both FRP and CP).* For the first time, the catalytic cycle, synergic effects, and the oxygen inhibition are theoretically confirmed to support the experimental hypothesis. The measured results of Mau et al are well analyzed and matching the predicted features of our modeling.

.
.   **Keywords:** polymerization kinetics; free radical, cationic polymerization, copper complex, photoredox catalyst.

1. Introduction

Light sources (lasers, LED or lamps) having light spectra ranging from UV (365 nm), visible (430 nm to 660 nm) to near infrared (750 nm to 950 nm) have been used for photopolymerization in both industrial and medical applications, such as dental curing, microlithography, stereolithography, microelectronics, holography, additive manufacturing, and 3D bioprinting [1-11]. Recently, copper complexes have been used as a new polymerization approach enabling the formation of acetylacetonate radicals by redox reaction to initiate the free radical polymerization (FRP) of acrylates

or the free radical promoted cationic polymerization (CP) of epoxides [12-16]. The efficiency of copper complex (G1) based photoinitiating systems (G1/iodonium salt (Iod)/*N*-vinylcarbazole (NVK)) was investigated by Mokbel et al [16], using light source (LEDs at 375, 395, 405 nm). Besides the experimental works [16], Lin et al [17] also developed kinetic modeling to analyze the G1/Iod/NVK systems.

However, in the G1 systems, most of the copper complexes have absorption peaks about 400 to 430 nm, which are still close to the ultraviolet spectrum having a small light penetration depth (few mm), comparing to that of visible light at about 500 nm (green) to 680 nm (red). A panchromatic light in visible (455 nm and 530 nm) were recently reported Mau et al [18] using two strategies, (i) modification of the electron donating substituent attached to the phenanthroline ligand; and (ii) introduction of a ferrocenyl group, in the bulky phosphorylated ligand, an iodonium salt (Iod) and ethyl 4-(dimethylamino)benzoate (EDB). Mau et al [18] investigated and compared the the system G1/Iod/EDB with the new copper complexes (defined as G2). They also compared the ferrocene-containing and ferrocene-free systems. Monomers of trimethylolpropane triacrylate (TMPTA) and (3,4-epoxycyclohexane)methyl-3,4- 301 epoxycyclohexylcarboxylate (EPOX) are used for FRP and CP, respectively, in the so called interpenetrated polymer network (IPN). Based on the measurements, Mau et al [18] have explored many new features and proposed or hypothesize mechanisms involved in the the dynamic profiles of the conversion efficacy. However, their phenomenological discussions are still lack of more precise conclusions which require a mathematical modeling as presented in this article.

As the second-part of our previous study of G2/IPN system, this article will present, for the first time, the kinetics and the conversion features of the 3-component system for the new copper complex (G2) initiator, based on our previous G1 system Mokbel et al [16] and Lin et al [17], and the new scheme proposed by *Mau* et al [18] for both FRP and CP. The roles of co-additive including their dual functions of regeneration of initiator and generation of extra radicals for improved conversion. The key factors influencing the conversion rates and efficacy will be explored by analytic formulas for the interpenetrated polymer network (IPN) capable of initiating both FRP and CP in a blend of trimethylolpropane triacrylate (TMPTA) and (3,4-epoxycyclohexane)methyl-3,4- 301 epoxycyclohexylcarboxylate (EPOX).

The measured data of *Mau* et al [18] will be quantitatively analyzed by our formulas, specially for the synergy effects (for improved FRP) from CP which could reduce the oxygen inhibition effects (on the free radicals) via the increase of oxygen viscosity. We will also analyze the role of the copper complex concentration, which is more sensitive for FRP than CP.

2. Methods and Modeling Systems

2.1. Photochemical kinetic schemes

As shown by Scheme 1, a 3-component system (A/B/N) defined by the ground state of initiator, [A], which is excited to its first-excited state PI*, and a triplet excited state T couples with an additive [B] to produce an oxidized-A (or [C]) and a radical R, which interacts with co-additive N to produce radical S'. Further coupling of S' and [C] produces another radical S and leads to the regeneration of [A]. Monomer M' and M coupled with radicals R and S' (for FRP) and S (for CP) conversion, respectively.
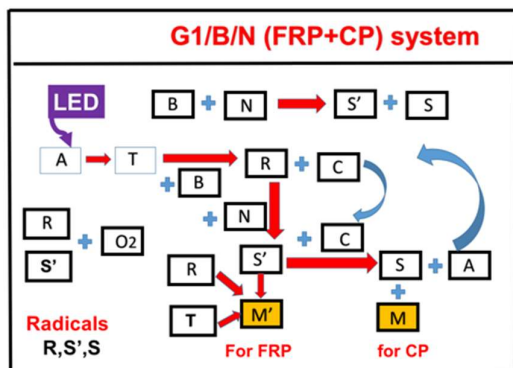
Scheme 1. The scheme chart of a 3-component system, (A/B/N), withe two monomers, M' and M, for the FRP and CP conversion, respectively, via radicals R, S' and S (see text for details).
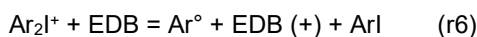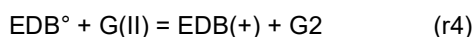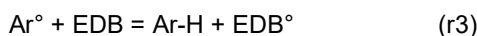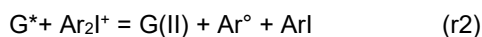
Specific measured system related to Scheme 1 was reported by Mokbel *et al [16] for a G1/Iod/amine system using a copper complex (G1). More recently, Mau* et al [18] proposed the photoredox catalytic cycle for a 3-component system of G2/Iod/EDB, where G2 is new copper complex based on our previous G1 structure, in combination with iodonium salt (Iod), (oxidizing agent) generates the radical species through an electron transfer reaction. The photoredox catalytic cycle for the three-component system G1/Iod/EDB is shown in Scheme 2 with the associated kinetic reactions shown in Scheme 3: (r1) for the light initiate copper complex (G2) to its excited triplet state G*; (r2) coupling of G* with Iod salt (Ar_2I^+) to produce oxodized-G2, or G(II), and radical Ar^o, which, in (r30, couples with EDB to produce radical EDB^o, which (r4) further couples with G(II) producing radical EDB(+) f and the regeneration of Ge; Also shown is the oxygen inhibition effect (r5). The charge transfer between EDB and amine (without the light excitation) producing radicals, S' and S, (r6).
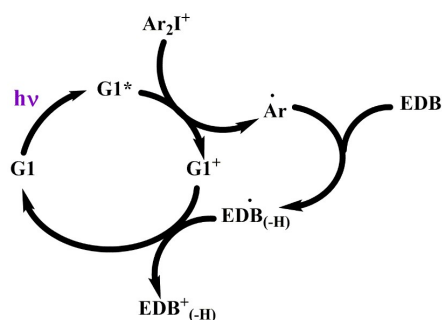
Scheme 2. Photoredox catalytic cycle for the three-component system G1/Iod/EDB - Adapted from [18].

The two-component system Iod/EDB was also used as a reference, in which EDB can form a charge transfer complex with the iodonium salt (Iod) producing radical EDB (+) for FRP, and radical Ar* for CP, without the light., shown by (r6) of Scheme 2. The oxygen inhibition (OIH) is shown in (r5). We will also discuss the synergy effects (for improved FRP) from CP which could reduce IOH via the increase of oxygen viscosity. Different from our previous model [17], the present article also includes the extra terms for OIH and the production of radicals S' and S from the charge transfer of EDB wit Iod.

We note that both radicals of Ar^o and EDB^o lead to FRP (in monomer TMPTA), and has a higher conversion efficacy than that of CP (in monomer EPOX), which is produced by only one radical EDB(+).

light + G2=G*   (r1)

G*+ Ar$_2$I$^+$ = G(II) + Ar° + ArI   (r2)

Ar° + EDB = Ar-H + EDB°   (r3)

EDB° + G(II) = EDB(+) + G2   (r4)

Ar° + O$_2$ = Ar-O$_2$* (r5)

Ar$_2$I$^+$ + EDB = Ar° + EDB (+) + ArI   (r6)

Scheme 3. The kinetic reactions for light initiated new copper complex (G2) for both FRP and CP conversation using radicals of Ar° and EDB° (for FRP), and radical EDB(+) for CP. Also shown are the regeneration of G2 in (r4) and the the oxygen inhibition effect in (r5) and the charge transfer between EDB and amine producing extra radicals, without the light initiation, (r6). See text for more details.

2.2. Formulas for conversion efficacy (CE)

The kinetic equations for our previous systems [17,19-21] are revised for the 3-component system (A/B/N) with 2-monomer M' (for FRP) andM (for CP) as follows.

$$\frac{d[A]}{dt} = - bI[A] + REG \tag{1}$$

$$\frac{d[B]}{dt} = -(k_2 T + K_{12}[N])[B] \tag{2}$$

$$\frac{dN}{dt} = -(k_6 R + K_{12}[B])N \tag{3}$$

$$\frac{dT}{dt} = bI[A] - (k_5 + k_2[B] + kM')T \tag{4}$$

$$\frac{d[C]}{dt} = k_2[B]T - k_4 S'[C] \tag{5}$$

$$\frac{dR}{dt} = k_2[B]T - (k"[O_2] + k_6 N + k'R + k_8 S' + k_7 M')R \tag{6}$$

$$\frac{dS'}{dt} = k_6 RN + K_{12}[B]N - (k_4[C] + K'M')S' \tag{7}$$

$$\frac{dS}{dt} = k_4[C]S' + K_{12}[B]N - KSM \tag{8}$$

In Eq. (1) the regeneration (REG) term of of the initiator, [A] given by REG= (k$_5$+k'M')T+ k$_4$[C]S'. b=83.6*a'wq*, where *w* is the light wavelength (in cm) and *q* is the triplet state T quantum yield; *a'* is the mole absorption coefficient, in (1/mM/%) and I (z, t) is the light intensity, in mW/cm^2. All the rate constants are defined previously [22] and they are related by the coupling terms. For examples, k$_j$ (with j=1,2) are for the couplings of T with [B] and [C], respectively; k$_4$ and k$_8$ are for the couplings of S' and [C], and R and M', respectively. The coupling of radicals R and S' with monomer M' (for FRP), and S with M (for CP) are given by the rate constants of K' and K, respectively. We have also include the oxygen inhibition (OIH) effect [23] (for system in air) given by the k"R[O$_2$} in Eq. (5). For system with laminate or when R is insensitive to oxygen (or k" is very small), OIH effect is redcued and conversion is improved [23]. In above kinetics, we have also include the bimolecular termination term, k$_7$R^2 in Eq. (6). Different from our previosu model, the present also includes the extra terms for oxygen and the production of radicals S' and S from the electron trnasfer between the amine and Iod. However the weak couplings of T and N, R and S are ignored.

The monomer conversions for FRP and CP are given by [19,20]

$$\frac{dM'}{dt} = -(kT + k'R + K'S')M' \qquad\qquad (9)$$

$$\frac{dM}{dt} = -KSM \qquad\qquad (10)$$

Above equations indicate that conversions for FRP and CP are given by the interaction of (T,R,S') and M', and S and M, respectively. We note that the co-initiator, [B] (or Iod) has dual function of enhancing FRP (via R and S') and CP (via S).

We note that Eq. (1) to (10) are constructed for the specific system of Mau et al [18], using short hand notations: A=Cu(I); T=Cu*(I), B=Iod; N=EDB, C= Cu(II), R= Ar*, S'= EDB°, S = EDB(+), in system having two monomers M'=TAMPTA (for FRP conversion) and M=epoxy (for CP conversion), where Iod is iodonium salt , EDB is N-vinylcarbazole, and TAMPA is trimethylol-propane triacrylate.

*2.2. Comprehensive form*ulas

For comprehensive formulas, we will use the so-called quasi-steady state assumption [19,20]. The life time of the singlet and triplet states of photosensitizer, the triplet state (T), and the radicals (R, S' and S), since they either decay or react with cellular matrix immediately after they are created. Thus, one may set dT/dt=dR/dt=dS'/dt = dS/dt=dC/dt= 0, which give the quasi-steady-state solutions: T=bIg[A], S'= [(K_{12}[B]+k_6R)N+ k_2T[B]]/(K'M'); S=(K_{12}N+k_2T)[B]/(KM); and g=1/(k_5+ k_2[B]+kM'). The oxygen inhibition effect, included in g' and S', reduces the free radicals, R and S', and hence the conversion of FRP and CP if system is in air. We have previously limited our formulas to the unimolecular coupling ok k'R [17]. However, the steady-state solution of Eq. (6) for R, is much complex due to the bimolecular coupling kR^2, and requires to solve Eq. (11) as follows.

$$k'R^2 + GR - H = 0 \qquad\qquad (11)$$

where G= k"[O_2] +k_6N+ k_7M', H= k_2[B]T; with T=bIg[A]. Solving for R, we obtain

$$R = \left(\frac{1}{2k'}\right)\left(-G + \sqrt{G^2 + 4k'H}\right) \qquad\qquad (12)$$

Case (i) for unimolecular termination dominant, or G>>k'H, we obtain R= k_2bIg([A][B]/G)(1-0.5H/G), which is an increasing function of H/G, or bIg[A][B]/G, for first-order with 0.5H<<G.
Case (ii) for bimolecular termination dominant, with H>> GR, we obtain, R=[H/k']^0.5, from Eq. (11), or more precisely, from Eq. (12),

$$R = \sqrt{H[1 + G^2/(8H^{0.5})]/k'} - G/(2k') \qquad\qquad (13)$$

We note that in both cases, R is a decreasing function of the oxygen inhibition effect (OIH), the k_5[O_2] in G. The OIH can be reduced via various strategies such as, Lin et al [21,22]: (i) using a pre-irradiation of a red-light to eliminate the oxygen; (ii) an additive which could convert the unstable oxidized molecule produced from the coupling of R and oxygen, to radicals; (iii) the synergy effect of FRP and CP in an interpenetrated polymer network (IPN) system which to be detailed more later.

Under the above quasi-steady-state solutions, we obtain the simplified equations as follows.

$$\frac{d[A]}{dt} = 0 \qquad\qquad (11)$$

$$\frac{d[B]}{dt} = -(k_2 bIg[A] + K_{12}N)[B] \qquad\qquad (12)$$

$$\frac{dN}{dt} = -(k_6 R + K_{12}[B])N \qquad\qquad (13)$$

where we have used the steady state condition, $k_4[C]S'= k_2[B]T$, and REG= $(k_5+k'M')T+k_4[C]S'$, reduces to REG= $(k_5+kM'+k_2[B])T$, we found that $Ib[A]$-RGE=0, a prefect catalytic cycle is available, such that [A] is a constant., $[A]=A_0$, We note that this REG enhances the conversion of FRP and CP, serving as a catalytic cycle.

The equation for the FRP and CP conversion rate functions are given as folows for two special cases.

For case (i) unimolecular dominant, R=H/G=$k_2[B]T/G= k_2$ ([B]T/(k'M'), with T=bIg[A].

$$\frac{dM'}{dt} = -kbIg[A]M' - 2k_2bIg[A][B] - (K_{12}[B] + k_6R)N \qquad (14)$$

$$\frac{dM}{dt} = - (K_{12}N + k_2bIg[A])[B] \qquad (15)$$

For case (ii) bimolecular dominant, $R=[H/k']^{0.5}$, we obtain

$$\frac{dM}{dt} = -- kbIg[A]M' - 2k'M'\sqrt{k_2bIg[A][B]/k'} - (K_{12}[B] + k_6R)N \qquad (16)$$

$$\frac{dM}{dt} = - (K_{12}N + k_2bIg[A])[B] \qquad (17)$$

The solution of above equations lead to the conversion efficacy (CE) defined by CE'=1- M'/M'_0 (for FRP), and CE=1- M/M_0 (for CP).

3.. Results and discussion

A full numerical simulation is required for the solutions of Eq. (11)-(17), which will be presenetd elasewhere. We will focus on comprehensive analysis for many features and the enhancement effects related to the measured data of Mau et al [18], based on the analytic solutions.

3.1 Analytic results

For analytic formulas, we will consider special cases of: (i) Iod/EDB system without light; (ii) G2/Iod system, with N=0; (iii) G2/Iod/EDB systems, and under the steady state condition which leads to a constant $[A]=A_0$, for a strong RGE.

Case (A). Without the light, the CE due to the reaction between EDB and Iod is given by, when bI=0, R=T=0, with steady state radicals given by S'=$K_{12}[B]N/(K'M')$; S=$(K_{12}[B]N/(KM)$, solution of $d[B]/dt=dN/dt=- K_{12}[B]N$ is N=B+d, with d given by the initial condistions of [B] and [N]; [B] may be found by approximately as: [B]=N-d=[Q - tK_{12}] = Q(1- K_{12}Qt), with Q= $B_0(1+ 0.5d/B_0)$, which is a decreasing function of time (t).

Therefore Eq. (15) and (16) become

$$\frac{dM'}{dt} = \frac{dM}{dt} = -K_{12}[B]N \qquad (18)$$

Time integral of [B]N, w eobatin M(t)=M_0 - P(t), with P(t)= Q(Q+d)t - 0.5(2Q+d)Q't² + 0.33Q'²t³, with Q'=K_{12} Q, and Q= $K_{12}B_0(1+ 0.5d/B_0)$, which is a nonlinear increasing function of time (t), and proprotional to K_{12} B_0 N_0. Therefore, the CE for FRP and CE' for CP are given by CE=1- M'/M'_0, CE=1- M/M_0, and both equals to P(t).

Case (B) for G2/Iod system, with N=0. With $[A]=A_0$, the first-order solutions of Eq. (2) is given by, [B]=B_0 -$IbtA_0$, for g=1/(k_5+ $k_2[B]$+k_2N+kM')= 1/($k_2[B]$), for kM'<<$k_1[B]$; Also G=k'M'; and for kT<<k'R, i.e, the first term of Eq. (14) for type-I, FRP is neglected. We obtain the following analytic solutions.

For case (i) unimolecular dominant, R=H/G, time integral of Eq. (14) gives the CE' (for FRP) =1- M'/M'$_0$, given by

$$CE(FRP) = 2k_2(bIA_0)t/M_0'$$ (19)

which is a linear incraesing function of time (t), for the case of N=0. Moreoverr, the CE for CP, given by Eq. (15) is half of CE (FRP), that is CE(CP=0.5 CE(FRP), for the case of N=0.

For case (ii) bimolecular dominant, $R=[H/k']^{0.5}$, time integral of Eq. (14) gives the CE for FRP as follows.

$$CE(FRP) = (1 - \exp[-H'(t)])/M_0'$$ (20)

$$H'(t) = 2k'\sqrt{(2/(3k')bIA_0}\ t^{1.5}$$ (21)

The CE(CP) has the same formula as CE(FRP), but with 0.5H'(t), in Eq. (19). We note that Eq. (19) is a highly nonlinear function of time, comparing to the a linear incraesing function of Eq. (18).

We also that above solutions are based on g=1/(k$_5$ +k$_2$[B]+k$_2$N+kM')= 1/(k$_2$[B]). We might have the condition that g=1/k$_5$, then [B]=B$_0$ exp(-dt), with d=(k$_2$/k$_5$)IbA$_0$. In this case, the CE becomes. Eq. (180 becomes

$$CE(FRP) = 2[1 - \exp(-dt)]$$ (22)

and CE(CP)=0.5 CE(FRP). Similarly, Eq. (19) becomes,

$$CE(FRP) = 1 - \exp[-H'(t)]$$ (23)

$$H'(t) = (4k'/\sqrt{dB_0})[1 - exp(-dt)]$$ (24)

which is consistent with our previous formulas [19,20], having the special feature that higher light intensity has a lower steady state valeu than that of lower intensity. These feature, based on g=1/k$_5$, does not exist in Eq. (22), or Eq. (19), (20) using g=1/(k$_2$[B]). THe CE(FRP) in Eq. (24) gives the CE(CP with H'(t) reduced to 0.5H'(t).

Case (C) for G2/Iod/EDB system. We need to solve for [B] and N from Eq. (11) and (12) first. WE will focus on the case that g=1/k$_5$. The first-order solution, with K$_{12}$[B]=0 in Eq. (11) gives [B]=B$_0$ exp(-dt), which is used to solve for Eq. (12), for the strong biomolecular case, with $R=[H/k']^{0.5}$, we obtain N(t)= N$_0$ exp[-(Q+Q')], Q=(k$_6$/k')dB$_0$H'(t), Q'= K$_{12}$B$_0$H'(t), with H'(t)=[1-exp(-dt)]/d. Solving for Eq. (16), and for H'(t)=dt, N(t)=N$_0$ exp[-(Q")t], with Q"=Q+Q', we obtain the CE for FRP as

$$CE(FRP) = 1 - \exp[-P(t)]$$

$$P(t) = H'(t)\,[1 + HOR]$$ (25)

where the high-orer term HOR is a complex function proportional to the time integarl of (K$_{12}$[B]+ k$_6$R)N, which needs numerical integration, having asteady state value proportional to [K$_{12}$B$_0$ + k$_6$ (A$_0$/Ib)$^{0.5}$] N$_0$. Solving for Eq. (15), we obtain the CE for CP given by Eq (25), but replacing P(t) to 0.5 P(t).

3.2 The synergic and enhancement effect in IPN system

3.2.1 Enhancement strategies

As reported by van der Laan et al. [4], the effectiveness of a photoinhibitor in a two-color system is strongly monomer-dependent, which also requires: (i) a high conversion of blue-photoinitiation in the absence of the UV-active inhibitor; (ii) a strong chain termination with significant reduction of blue and UV conversion in the presence of UV-active inhibitor and (iii) short induction time or rapid elimination of the inhibitor species in the dark (or absence of UV-light) [22]. Conversion efficiency may be also improved by reduction of the oxygen inhibition effect [23]. Synergic effects have been reported using co-initiator and/or additives and 2- and 3-wavelength systems [8,10]. The present article presents the kinetics analysis of the co-additive enhanced (catalyzed) conversion in FRP and CP which was reported by Mokbel et al [19], Garra et al [20] and Noribnet et al [21] in the 3-compnent G1/Iod/NVK system.

3.2.2 Synergic effects in IPN

The synergy effects (for improved CE) in an interpenetrated polymer network (IPN) system were discussed by Mau et al [18] for the polymerization of a TMPTA/EPOX blend in the presence of G2/Iod/EDB. Three factors were proposed as follows.

(i) The FRP is at first inhibited by the oxygen in the medium, the OIH effects. However, while the cationic polymerization (CP) starts immediately which increase of the medium viscosity limiting the diffusional oxygen replenishment, such that OIH is reduced; (ii) The cationic monomer also acts as a diluting agent for the radical polymer network allowing to achieve a higher conversion. (iii) the exothermic property of the radical polymerization also tends to boost the cationic polymerization that is quite temperature sensitive. As shown by Eq. (12) an (13), the radical (R) is reduced by the OIH term $k_5[O_2]$ in G. This OIH effects also supresses the CE of FRP, specialy for the transient profile (till the oxygen is completely depleted). We note that this OIH does not affect the CE of CP, given by the radical S, which is independent to oxygen. This theoretical prediction was justified by the mearsued work of Mokbel et al [19], they reported that the radical for CP is much less sensitive to OIH than that of FRP. Mokbel et al [19] showed the OIH for system in air and in lamine, showing that the FRP conversion of TMPTA was higher in laminate than in air. In contrast, the CP conversion of epoxy function was lower in laminate than in air. It may be because the FRP of TMPTA was faster than the CP, and most of the free radicals were consumed to initiate FRP.

3.3 Roles of copper complex (G2) concentrations

Mau et al [18] reported that, in their Table 2 for G2/Iod/EDB system with TMPTA/EPOX monomer, the impact of the 10-fold reduction of copper compex (G2) initial concentration (from 0.7% to 0.07%) is particularly high on the CE of cationic polymerization (CE rediced from 51% to 30%). In contrast, it has much less impacting the free radical polymerization (CE reduced from 86% to 82%). This unique feature confirms our hypothesis on the IPN reactivities as photocatalysts in a photoredox cycle like G1. Mathematically, this could be realized by the REG term for regeneration of the initiaator ([A] or, G2), in our Eq. (1), in which for the strong RGE case, $bI[A]=RGE$, such that [A] is kept as a constant via the continuing regenerationn of A_0.

The more sensitive dependence of CP than that of FRP on the G2 concentration (A_0) may be realized by comparing Eq. (14) and (15) as follows. Eq. (14) for FRP is attributed from 3 coupling terms: the type-I T and M' coupling, the R and M' coupling and the T and N couplng. The $K_{12}[B]N$ term is for the CE of Iod/EDB (without the light), which is higher in FRP than CP, and it is independent to G2 initial concentration (A_0). Eq. (15) shows the CE for CP, in which $K_{12}N$ is smaller than $k_2bIg\{A]$ which has a strong A_0 dependence. Therefore, the CE of CP is also strongly dependent on A_0, In comparison, for the CE of FRP, Eq. (14) has a rather high efficacy from the

$K_{12}[B]N$ term, as shown by Fig. 5A of Mau et al [18], and it is not affected by A_0. Therfore, the impact of A_0 on the $k_2bIg\{A\}$ term of FRP is not as strong as that of CP. Moreover, for higer CE in FRP, the saturated value is les sensive to A_0. We have previously theorized the optimal concentration for maxiumum efficacy [20]. Moreover, we note that the catalytic cycle from the regenaration of the initiator [A] should also play important role, such that a small amount of initial G2 concentration (0.07%) is capable of being recycled for hogh efficacy, specially for FRP. However, the theortically predicted optimal concentrations [20] for G2, Iod and EDM remain to be explored experimentally.

3.4 General features and new findings

As shown by Eqs. (14) and (15), and the approximated solution of Eq. (18) to (22), the following significant features of the system G2/Iod/EDB in monmer blend of TMPTA/EPOX are summarized.

(a) Under the steady state condition, $bI[A]=RGE$ in Eq. (1), and $d[A]/dt=0$, which leads to a prefect catalytic cycle such that [A] is a constant., $[A]=A_0$, We note that the REG enhances the conversion of FRP and CP, serving as a catalytic cycle. Without RGE (or a nonperfect RGE), [A] is depleted during the photopolmerization, given by a format of $[A]=A_0 Exp(-dt)$, leading to a lower staedy state efficacy for bot FRP and CP, unless there is a contnuing supply of the initiator, such as in the clincal protocal of corneal crosslinking procedure, where more riboflaving solution drops are added during the procedure [19].

(b) Both radicals of R (or Ar^o) and S' (or EDB^o) lead to FRP (in monomer TMPTA), and has a higher conversion efficacy than that of CP (in monomer EPOX), which is produced by only one radical S (or EDB(+)). As shown by Eq. (14) and (15), the rate function of FRP is about twice of CP, when N=0. In the presence of N (or EDB), efficacy increases due to the coupling terms of $K_{12}NT$ in both FRP and CP.

(c) Co-additicve [B] has multiple functions of : (i) regeneration of initiator [A] leading to higher FRP and CP conversion; (ii) producing of radical S'(for FRP), and (iii) producing radical S (for CP), via the re-coupling with radical [C], produced by[B].

(d) Co- additicve [N] has functions of : (i) generation of S' for FRP; and (ii) generation of cationic radical S for CP conversion; via $k_6R[N]$. Our analytic formulas show that CE (of CP) is bout 0.5 of CE(of FRP), as shown by Eq. (18) to (24).

(e) The oxygen inhibition (OIH) effect (or the term $k''[O_2]$), reduces the free radicals R and S', and thus the FRP conversion, which is lower in air comparing to in laminate [23]. However, the OIH effect has much less impact on the CE of CP, as also demonstrated by Mau et al [18] experimently.

(f) In the IPN system, the synergic effects due to the co-exist of FRP and CP include: (i) CP can increase the medium viscosity limiting the diffusional oxygen replenishment, such that OIH is reduced; (ii) the cationic monomer also acts as a diluting agent for the radical polymer network , and (iii) the exothermic property of the radical polymerization also tends to boost the cationic polymerization that is quite temperature sensitive. We note that the overall efficacy of both FRP and CP ate improved via the above described synergic effects, and most importaly, via the catalytic cycle from the regenaration of the initiator [A], the RGE term in Eq. (1) which leads to a constant [A], when RGE =bI[A], such that $d[A]/dt=0$. The present model, for the first time, confirmed mathematically this importnat faeture, which was hypothesized by experimentalists [18].

(g) We note that the catalytic cycle from the regenaration of the initiator [A] should also play important role in the dependence of efficacy on the copper complex (G2) concentrations, such that a small amount of initial G2 (0.07%) is capable of being recycled for high efficacy, specially for FRP, as hypothesized experimentally [18]. However, the theortically predicted optimal concentrations [20] for G2, Iod and EDM remain to be explored experimentally.

4. Conclusion

This article presents, for the first time, the kinetics and the general conversion features of the interpenetrated polymer network (IPN) capable of initiating both FRP and CP in a blend of TMPTA and EPOX, as the monomer for FRP and CP, respectively. The synergic effects due to CP include: (i) the increased viscosity (via CP) limiting the diffusional oxygen replenishment, such that OIH are reduced; (ii) the cationic monomer also acts as a diluting agent for the IPN network , and (iii) the exothermic property of the CP. The new findings based on our formuals include: (i) the CE of FRP is about twice of the CE of CP, due to the extra radicals involved in FRP; (ii) the catalytic cycle enhancing the efficacy is mainly due to the regenaration of the initiator, the RGE term in Eq. (1) which leads to a constant under the steady-state conditions, such that RGE = bI[A], or d[A]/dt=0; (iii) the nonlinear dependence of light intensity of the CE (in both FRP and CP). For the first time, the catalytic cycle, synergic effects, and the oxygen inhibition are theoretically confirmed to support the experimental hypothesis [18]. *The measured results of Mau et al are well analyzed and matching the predicted features of our modeling.*

Conflicts of Interest: Jui-Teng Lin is the CEO of New Vision Inc.

References

1. Fouassier, J. P. & Lalevée, J. Photoinitiators for Polymer Synthesis-Scope, Reactivity and Efficiency. Wiley-VCH Verlag GmbH & Co. KGaA: Weinheim, Germany, 2012.

2. Yagci, Y., Jockusch, S. & Turro, N.J. Photoinitiated polymerization: Advances, challenges and opportunities. *Macromolecules* **43**, 6245–6260 (2010).

3. de Beer, M.P.; van der Laan, H.L.; Cole, M.A.; Whelan, R.J.; Burns, M.A.; Scott, T.F. Rapid, Continuous Additive Manufacturing by Volumetric Polymerization Inhibition Patterning. *Sci. Adv.* **2019**, *5*, 8.

4. van der Laan, H.L.; Burns, M.A.; Scott, T.F. Volumetric Photopolymerization Confinement through Dual-Wavelength Photoinitiation and Photoinhibition. *ACS Macro Lett.* **2019**, *8*, 899–904.

5. Childress, K.K., Kim, K., Glugla, D.J., Musgrave, C.B., Bowman, C.N. & Stansbury, J.W. Independent control of singlet oxygen and radical generation via irradiation of a two-color photosensitive molecule. Macromolecules **52**(13):4968–4978 (2019).

6. Scott, T.F.; Kowalski, B.A.; Sullivan, A.C.; Bowman, C.N.; McLeod, R.R. Two-Color Single-Photon Photoinitiation and Photoinhibition for Subdiffraction Photolithography. *Science* **2009**, *324*, 913–917.

7. Kirschner, J.; Paillard, J.; Bouzrati-Zerell, M.; et al. Aryliodonium ylides as novel and efficient additives for radical chemistry: example in camphorquinone (CQ)/Amine based photoinitiating systems. *Molecules* **24**(16), 2913 (2019); doi:10.3390/molecules24162913.

8. Bonardi AH,; Dumur F,; Grant TM,; et al. High performance near-Infrared (NIR) photoinitiating systems operating under low light intensity and in the presence of oxygen. Macromolecules, 2018, 51, 1314-1324.

9. Lin, J.T.; Liu, H.W.; Chen, K.T.; Cheng, D..C. 3-wavelength (UV, blue, red) controlled photopolymerization: improved conversion and confinement in 3D-printing. IEEE Access, 2020, 8, 49353-49362.

10. Lin, J.T.; Chen, K.T.; Cheng D.C.; Liu, H,W. Enhancing blue-light-initiated photopolymerization in a three-component system: kinetic and modeling of conversion strategies. J Polymer Research, 2021, 28:2.

11. Pigot, C.; Noirbent, G.; Brunel, D.; Dumur, F. Recent advances on push-pull organic dyes as visible light photoinitiators of polymerization. *Eur. Polym. J.* **2020**, *133*, 109797.

12. Alzahrani, A.A.; Erbse, A.H.; Bowman, C.N. Evaluation and development of novel photoinitiator complexes for photoinitiating the copper-catalyzed azide-alkyne cycloaddition reaction. *Polym. Chem*. **2014**, *5*, 1874–1882.

13. Xiao, P.; Dumur, F.; Zhang, J.; Fouassier, J.-P.; Gigmes, D.; Lalevée, J. Copper complexes in radical photoinitiating systems: Applications to free radical and cationic polymerization under visible lights. *Macromolecules* **2014**, *47*, 3837–3844.

14. Garra, P.; Dietlin, C.; Morlet-Savary, F.; Dumur, F.; et al Redox two-component initiated free radical and cationic polymerizations: Concepts, reactions and applications. Progress in Polymer Science, 2019, 94, pp.33–56. 10.1016/j.progpolymsci.2019.04.003

15. Noirbent, G.; Dumur, F. Recent Advances on Copper Complexes as Visible Light Photoinitiators and (Photo) Redox Initiators of Polymerization. Catalysts, MDPI, 2020, 10, 10.3390/catal10090953 .

16. Mokbel, H.; Anderson, D.; Plenderleith, R.; Dietlin, C.; et al. Copper photoredox catalyst "G1": A new high performance photoinitiator for near-UV and visible LEDs. *J. Polym. Chem*. **2017**, *8*, 5580–5592.

17. Lin, J.T,; Laleee, J.; Cheng, D.C. Kinetics analysis of copper complex photoredox catalyst: roles of oxygen, thickness, and optimal concentration for radical/cationic hybrid photopolymerization. *Preprints* **2021**, 2021050597.

18. Mau, A.; Mokbel, H.; Dietlin, C.; Graff, B.; et al. Panchromatic Copper Complexes for Visible Light Photopolymerization. Photochem. 2021 (in press).

19. Lin, J.T,; Cheng, D.C. Modeling the efficacy profiles of UV-light activated corneal collagen crosslinking. PloS One. 2017;12:e0175002.

20. *Lin, .JT.; Liu, H.W.; Chen, K.T.; Cheng, D.C.* Modeling the optimal conditions for improved efficacy and crosslink depth of photo-initiated polymerization. Polymers. 2019, 11, 217; doi:10.3390/polym11020217.

21. Lin J.T.; Liu HW,; Chen KT,; Chiu YC, ; Cheng DC. Enhancing UV photopolymerization by a red-light pre-irradiation: kinetics and modeling strategies for reduced oxygen-inhibition. J Polymer Science, 2020，58， 683-691，DOI:10.1002/pol.20190201.

22. Lin, J.T,; Lalevee, L.; Cheng. D,C. Synergetic kinetics of free radical and cationic photopolymerization in three co-initiators and two-monomers system. Polymers (2021, in press).

23. Lin, J.T,; Chen. K.T,; Cheng. D,C,; Liu. H,W. Modeling the efficacy of radical-mediated photopolymerization: the role of oxygen inhibition, viscosity and induction time. *Front. Chem. 2019, 7:760. doi: 10.3389/fchem.2019.00760.*